

Automating Mushroom Culture Classification: A Machine Learning Approach

Hamimah Ujir¹, Irwandi Hipiny², Mohamad Hasnul Bolhassan³, Ku Nurul Fazira Ku Azir⁴, SA Ali⁵

Faculty of Computer Science and Information Technology, Universiti Malaysia Sarawak, Sarawak, Malaysia^{1,2}

Faculty of Resource Science and Technology, Universiti Malaysia Sarawak, Sarawak, Malaysia³

Faculty of Electronic Engineering & Technology, Universiti Malaysia Perlis, Malaysia⁴

Faculty of Artificial Intelligence & Mathematical Sciences, SMIU, Karachi-74000, Pakistan⁵

Abstract—Traditionally, the classification of mushroom cultures has conventionally relied on manual inspection by human experts. However, this methodology is susceptible to human bias and errors, primarily due to its dependency on individual judgments. To overcome these limitations, we introduce an innovative approach that harnesses machine learning methodologies to automate the classification of mushroom cultures. Our methodology employs two distinct strategies: the first involves utilizing the histogram profile of the HSV color space, while the second employs a convolutional neural network (CNN)-based technique. We evaluated a dataset of 1400 images from two strains of *Pleurotus ostreatus* mycelium samples over a period of 14 days. During the cultivation phase, we base our operations on the histogram profiles of the masked areas. The application of the HSV histogram profile led to an average precision of 74.6% for phase 2, with phase 3 yielding a higher precision of 95.2%. For CNN-based method, the discriminative image features are extracted from captured images of rhizomorph mycelium growth. These features are then used to train a machine learning model that can accurately estimate the growth rate of a rhizomorph mycelium culture and predict contamination status. Using MNet and MConNet approach, our results achieved an average accuracy of 92.15% for growth prediction and 97.81% for contamination prediction. Our results suggest that computer-based approaches could revolutionize the mushroom cultivation industry by making it more efficient and productive. Our approach is less prone to human error than manual inspection, and it can be used to produce mushrooms more efficiently and with higher quality.

Keywords—Machine learning; convolution neural networks; mushroom cultivation; rhizomorph mycelium

I. INTRODUCTION

Mushroom cultures can be initiated from either spores or tissue [1]. The choice of whether to initiate a mushroom culture from spores or tissue depends on several factors, including the type of mushroom being grown, the desired yield, and the level of control that the cultivator wants to have over the culture. When dealing with spores, one must choose a single strain from the numerous strains produced. Conversely, tissue culture enables the cultivator to preserve the precise genetic makeup of the parent mushroom. In either scenario, the outcome is a network of cells collectively referred to as the mushroom mycelium. According to study [2], there are two main forms of mushroom mycelium which are: rhizomorph mycelium and tomentose mycelium. The rhizomorph mycelium resembles

plant roots, and only the growing rhizomorph mycelium is utilized for subsequent cultivation.

According to study [3], mushroom cultivation needs a lot of labor. The standard practice for selecting mushroom culture for further cultivation is via eye inspection by an expert. This method depends on human experts, making it susceptible to human bias and errors. The expert classifies rhizomorph and fluffy growing mycelium by examining the "fluffiness" of the sample under a lamp while holding the petri dish. Intensive training is thus required for a worker/newcomer in this field to learn how to select the fast-growing rhizomorph mycelium and estimate the right moment to transfer the culture to an agar petri dish. The fastest-growing rhizomorph mycelium is selected and transferred to another agar petri dish. Those exhibiting slower growth rates or contamination are subsequently discarded. This is where the skill of mushroom growers comes into play, as they must discern the quality and the optimal moment to harvest the rhizomorph mycelium for cultivation in a petri dish. Note that mushroom mycelium can grow exponentially, achieving a mass thousands of times its original size. Choosing a quality rhizomorph mycelium is particularly important to ensure a sizeable harvest.

We propose a computer vision approach in conjunction with a machine learning model. This would leverage discriminative image features to quickly identify growing rhizomorph mycelium cultures and ascertain the ideal timing for their transfer to an agar petri dish. Our objective is to differentiate fast-growing rhizomorph mycelium cultures from the ones with a slower growth rate. This paper also discusses the prediction of rhizomorph mycelium growth based on its diameter and identifies the good and bad mycelium.

Section II examines prior research that has employed computer-based technology in mushroom farming and Section III describes the process of collecting data for this study. Section IV presents the methods used for predicting growth rate and identifying good and bad mycelium and Section V presents the results of this study. Finally, Section VI concludes the paper.

II. RELATED WORKS

Computer-based solutions in the field of mushroom cultivation mainly focus on two areas: recognizing edible mushroom types and monitoring mushroom growth using

computer assisted technology such as the Internet of Things (IoT).

Several studies centered on mushroom classification include [4]-[10]. The study in [4] classified mushrooms into two categories, poisonous and non-poisonous using different algorithms like neural network (NN), Support Vector Machines (SVM), Decision Tree, and k Nearest Neighbors (kNN). They utilized a dataset comprising mushroom images, which includes images with and without backgrounds. Experimental findings reveal that the most effective technique for classifying mushroom images is kNN, achieving an accuracy of 94% when utilizing features extracted from images with real dimensions of mushroom types, and 87% when using features extracted solely from images. The research in [5] proposes a new model of classifying 45 types of mushrooms including edible and poisonous mushrooms by using a technique of Convolution Neural Networks (CNN). They used the library KERAS2.3.1 for running the CNN TensorFlow and the proposed model gives the results of 0.78, 0.73, and 0.74 for precision, recall, and F1 score, respectively. The study in [7] used deep learning approaches like InceptionV3, VGG16 and Resnet50 to identify the mushrooms based on their category on 8190 mushroom images where the ratio of training and testing data was 8:2. They used The Contrast Limited Adaptive Histogram Equalization (CLAHE) method along with InceptionV3 to obtain the highest test accuracy. InceptionV3 achieved the highest accuracy of 88.40% among the implemented algorithms. The research in [8] conduct a comparison between the performance of Random Forest and Reduced Error Pruning (REP) tree classification algorithms in classifying edible and poisonous mushrooms. The study in [9] employed Gaussian naïve Bayes along with Linear Discriminant Analysis (LDA) to separate edible and non-edible mushrooms. LDA was used to reduce the dataset, which helped in reducing the dimensionality of the feature space and removing irrelevant features. LDA aims to enhance the distinction between various classes by identifying a linear combination of features that most effectively discriminates among them. A slightly different work by [10] where they utilize K Means clustering algorithm to classify mushrooms based on attributes such as structure, surface size, cap tone, gill, stalk, smell, place of growth, and population. From their study, it is evident that the odor attribute stands out as the most significant factor contributing to the highest classification accuracy.

In study [11] proposed an IoT-based monitoring and control system for shiitake mushroom farms using wireless sensors. According to study [11], implementing IoT technology in mushroom farms presents challenges such as energy management, data security, sensor node placement, internet connectivity, and transmission range. The research in [12] designed a smart system called SENSEPACK to monitor the environment of a mushroom cultivation farm. This system measures temperature, humidity, light, and CO₂ levels using appropriate sensors to control the environment of the nursing room.

Recently, there has been a notable increase in endeavors to automate mushroom cultivation in controlled environments, utilizing not only IoT but also mobile applications, such as [13] [14]. The study in [13] proposed a solution utilizing an

Android app was proposed to distinguish between edible and poisonous mushrooms. In this work, machine vision and CNN classification algorithm is used to develop the app. The automation system introduced by utilizing sensors within the mushroom house guarantees ideal conditions for the growth of mushroom.

Other than that, the study in [15] presented a novel approach in the mushroom cultivation field, utilizing computer-assisted technology to classify mushroom samples based on the enzymatic browning reaction. This reaction occurs when mushrooms are exposed to the atmosphere, and the proposed method employs a support vector machine (SVM) classifier to achieve a classification accuracy of 80%. The research in [16] employs a dataset sourced from Kaggle for mushroom classification and model training purposes. They apply methods such as SVM, naïve Bayes, and random forest algorithms in this study. Their findings reveal that their data is prone to overfitting, attributed to its near-linear separability as observed through the principle of SVM. Another similar work by [17] used decision tree to classify five types of mushrooms, they are Button mushrooms, Wood Ear mushrooms, Straw mushrooms, Reishi mushrooms and Red Oyster mushrooms. Among the feature extracted from the mushroom images are mean, skewness, variance, kurtosis, and entropy from the mushroom images.

In general, deep learning techniques are also employed in the other agricultural sector to categorize, quantify, and partition the areas of significance pertaining to crops. The study in [18] published a dataset that uses deep-learning-based classification and detection in precision agriculture. CropDeep consists of 31,147 images with over 49,000 annotated instances from 31 different classes. Based on the results, they suggested that the YOLOv3 network has good potential application in agricultural detection tasks. The study in [19] proposes a deep learning-based solution for object detection in Smart Agriculture. The solution can automatically detect damage in leaves and fruits, locate them, classify their severity levels, and visualize them by contouring their exact locations. Their results reveal that the proposed solution which is based on Mask-RCNN, achieves higher performances in features extraction and damage detection/localization compared to other pre-trained models such as VGG16 and VGG19. Another different work proposed by [20] works on algorithm to classify wild mushrooms using a deep CNN and Residual Network [20] also introduces an optimization method that improved the classification effect of the algorithm model, enhancing the overall performance of the classification algorithm

Based on our current understanding of the literature, there has been no prior investigation into the use of histogram profiles and machine learning approach for the recognition of fast-growing rhizomorph mycelium through the analysis of image features. As a result, the research problem we are currently pursuing represents an unexplored area of inquiry within this field.

III. DATA COLLECTION

Two strains are used in the experiments, and both are *Pleurotus ostreatus*. A disk of mycelium of 5 mm diameter was placed in the center of a Petri dish containing Potato-

Dextrose-Agar (PDA) medium. During the spawn-run (development and growing of the mycelium) the sealed Petri dishes are stored in a dark and neat place. Petri dishes with fungi were numbered for identification. Each strain has about fifty samples.

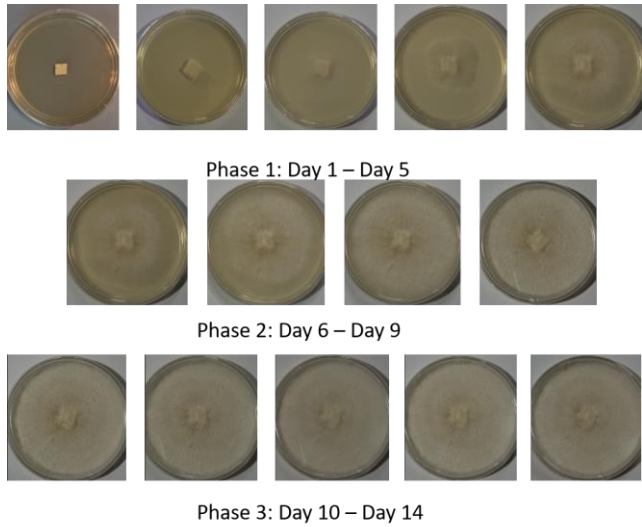


Fig. 1. The growth of a good rhizomorph mycelium in 14 days.

An android camera phone mounted on a tripod. Images of Petri dishes with mycelia were obtained against a white background and identified with a paper label of a known area of 4 cm² (2 x 2 cm). Photographs were taken daily for fourteen days for both strains, totaling 1400 images. Fig. 1 shows a sample of a good rhizomorph mycelium sample in 14 days. There are three phases (classes) used to categorize the growth of mycelium: Phase 1 (Day 1 – Day 5); Phase 2 (Day 6- Day 9) and Phase 3 (Day 10 - Day 14). From the observation of the sample, the growth is quite drastic in phase 2. During phase 3, the growth is the same for the last five days and human eyes cannot easily observe the difference for each day. Human eyes can also make mistakes during the last two days in phase 2, as it can be mistakenly labeled as phase 3.

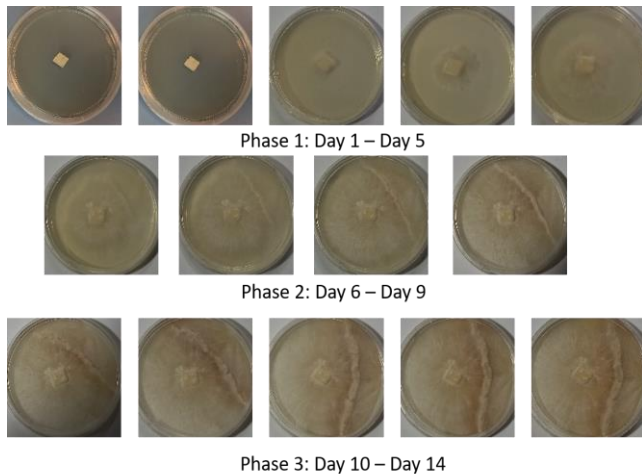


Fig. 2. The growth of a contaminated rhizomorph mycelium in 14 days.

Fig. 2 shows a sample of a contaminated rhizomorph mycelium sample in 14 days. During phase 1, the good and contaminated mycelium cannot be differentiated, as it grows the same. However, during phase 2, the contaminated one can be easily recognized on day 7. Like good mycelium, during phase 3, the growth of the contaminated one is the same for the last five days.

IV. METHOD

A. Classification Based on HSV Histogram Profile

For rhizomorph mycelium growth analysis measurement, mask ROI segmentation and elimination is used to determine the cultivation of the phases. The proposed method determines the cultivation phase based on the mask area's histogram profile. Given a top-view and close-up image of the petri dish sample, we obtained n candidate mask(s) using Hough circles. We set the min circle radii to a default value of 1400px to exclude smaller circles. The default threshold value was determined heuristically from random sample images of our dataset. Next, we build a 2D HSV histogram map (30 hue bins x 32 saturation bins) for each candidate mask. Three examples of such maps are shown in Fig. 3. The intensity value of each cell represents the frequency of occurrence of that hue-saturation combination for that image. A lighter shade indicates a higher peak and vice versa.

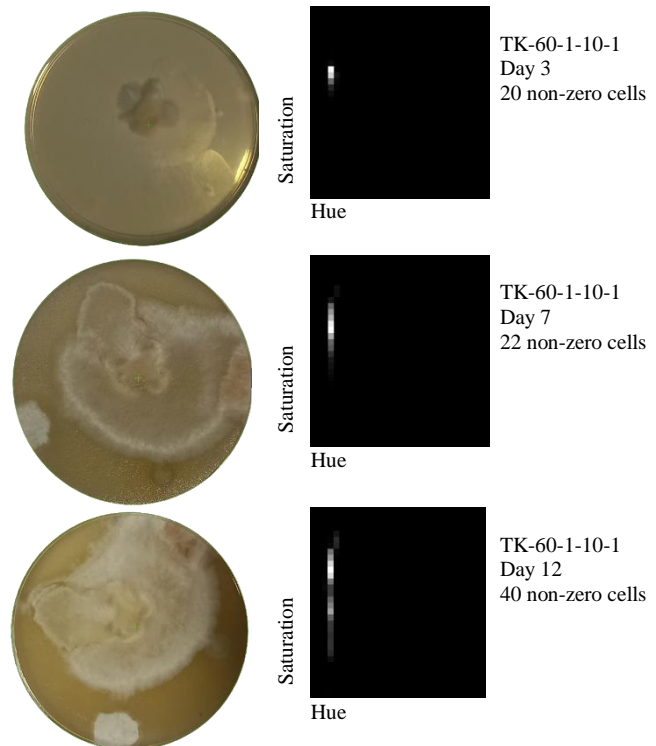


Fig. 3. 2D HSV histogram maps, each produced from the final mask of an image belonging to TK-60-1-10-1. The three images were captured on Day 3, Day 7 and Day 12, respectively. We also reported the number of non-zero cells for comparison.

We eliminate a mask candidate if it returns a high entropy value since it is more likely to be produced due to a segmentation error. The segmented area includes background pixels (i.e., petri dish and desk surface) hence the higher

variety of hue-saturation combinations. The mask candidate with the lowest entropy value (i.e., the lowest number of non-zero cells) is thus retained as the final mask.

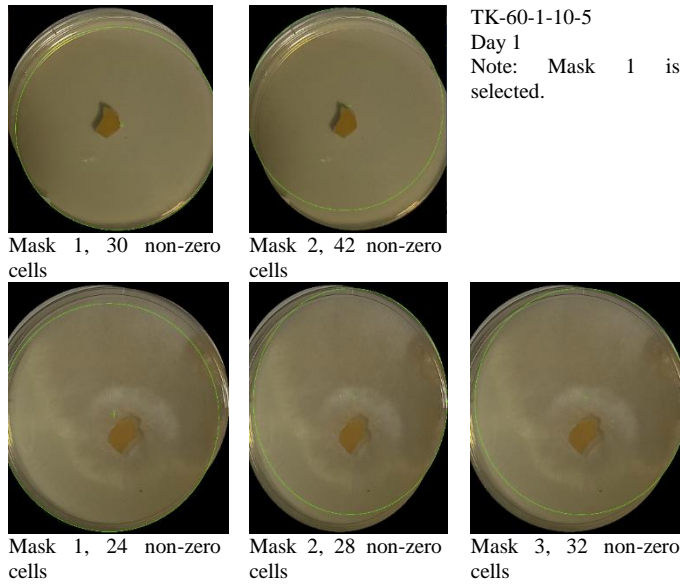


Fig. 4. Two instances of the segmentation function returning $n > 1$ mask candidates. The mask area is enclosed inside the green-colored circle.

Fig. 4 shows two instances of our mask ROI segmentation function returning multiple candidates. The number of non-zero cells for each candidate is reported for comparison. Mask candidates with more non-zero cells tend to include many background pixels. For TK-60-1-10-5, mask number 2 was rejected since the Hough circle encloses a larger portion of the petri dish rim than mask number 1. For TR-60-1-20-20, the decision is not as clear-cut since all three masks enclose (with varying degrees) some parts of the rim. Nevertheless, mask number 1 was chosen because it contains the least non-zero cells. Images with no mask detected are discarded. Such cases are typically due to poor image quality during capture.

Given a 2D HSV histogram map, M_i our method determines the specimen's label by counting the number of non-zero cells, $NZERO(M_i)$, with an intensity value exceeding the set threshold, $thresh$. We then compute the absolute difference between the counted value and two constants, i.e., lower bound, $LBOUND$, and upper bound, $UBOUND$. Value for each constant was determined from our training set, either using Median, Mod or Average. The first constant represents the NON-CONTAMINATED set (i.e., lower entropy), and the latter represents the CONTAMINATED set (i.e., higher entropy). Thus, the formula to obtain the final classification label, i.e., CONTAMINATED, C, vs. NON-CONTAMINATED, NC, is given below,

$$LABEL(M_i) = \begin{cases} C, & \text{if } |NZERO(M_i) - LBOUND| \geq |NZERO(M_i) - UBOUND| \\ NC, & \text{otherwise} \end{cases} \quad (1)$$

For phase determination, we limit the test dataset to NON-CONTAMINATED only since contaminated specimens are almost impossible to classify due to their chaotic appearance. We determine the phase label as a distance function between

the current image's non-zero cell count and the LBOUND value of each phase,

$$PHASE(M_i) = \begin{cases} 1 & \text{if } |NZERO(M_i) - LBOUND_2| > |NZERO(M_i) - LBOUND_1| < |NZERO(M_i) - LBOUND_3| \\ 2 & \text{if } |NZERO(M_i) - LBOUND_1| > |NZERO(M_i) - LBOUND_2| < |NZERO(M_i) - LBOUND_3| \\ 3 & \text{otherwise} \end{cases} \quad (2)$$

B. Classification using CNN-based Method

On top of the previous method, CNN-based method was also chosen to analyze the images of the mushroom. Using machine learning does not require handcrafted feature analysis and it performs feature analysis within the network. There are two neural networks used to predict the growth rate and contamination of the mushroom named MNet and MConNet respectively (see Fig. 5). The underlying architecture for both neural networks is similar except for the activation function for the last layer such that the final layer of the neural network is using SoftMax for MNet while using sigmoid for MConNet.

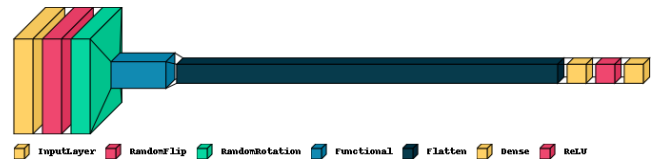


Fig. 5. The architectural diagram for MNet and MConNet.

The architecture of both models is utilizing transfer learning from MobileNetV3 due to its acceptable performance in low-end mobile devices and possible real-time prediction. Moreover, there are two layers such as *RandomFlip* and *RandomRotation* for generalizing the samples and preventing overfitting during the training. The side-effect of this also virtually increases the number of samples. Though similar, both the neural networks can be combined for improvement in performance and latency. However, the method described is not feasible when there are mixes of contaminated and non-contaminated images in the training samples.

A total of 1400 samples collected earlier are split into 64%, 16%, and 20% for training, validation, and testing, respectively. The samples were trained through TensorFlow by minimizing sparse categorical cross entropy for MNet and binary cross-entropy for MConNet. The trained models were evaluated with testing samples that are not included in the training samples.

V. RESULTS AND ANALYSIS

In this section, we explained the results in two parts: (a) rhizomorph mycelium contamination recognition; and (b) growth analysis measurement using two different methods as explained in the previous section.

A. Classification Based on HSV Histogram Profile

To discover the optimal lower and upper bound values, we clustered all images belonging to 30 training specimens according to phases, i.e., Phase 1 (Day 1 – 5), Phase 2 (Day 6 – 8), and Phase 3 (Day 9 – 12), and classification labels. We obtained each cluster's median, mod, and average non-zero cell count under each intensity threshold value. The results are tabulated in Table I.

TABLE I. LBOUND AND UBOUND VALUES FOR EACH CLUSTER VS. METRIC COMBINATION

Cluster	Metric	Number of non-zero cells with intensity value exceeding threshold					
		>0		>64		>128	
		NC	C	NC	C	NC	C
PHASE 1	Median	26.0	29.0	4.0	5.0	3.0	3.0
	Mod	23.0	30.0	3.0	4.0	2.0	2.0
	Average	26.0	28.6	4.8	5.0	3.0	3.2
PHASE 2	Median	20.0	29.0	5.0	8.0	3.0	5.0
	Mod	16.0	25.0	5.0	8.0	2.0	5.0
	Average	22.5	32.9	6.1	8.1	3.4	4.8
PHASE 3	Median	19.0	33.5	5.0	7.0	3.0	4.0
	Mod	17.0	27.0	5.0	6.0	3.0	4.0
	Average	21.2	36.0	5.6	7.9	3.4	4.6

1) *Rhizomorph mycelium contamination recognition*: We report the average precision of each combination to predict the specimen's label (CONTAMINATED vs. NON-CONTAMINATED), see Fig. 3, on a test set containing never-seen-before images of 20 specimens. The test set contains ten contaminated and ten non-contaminated specimens. We contrast the results obtained when making the prediction based on Phase 2's images (n=63) vs Phase 3's images (m=72). We exclude Phase 1's images as contamination signs only start to appear from Phase 2 onwards.

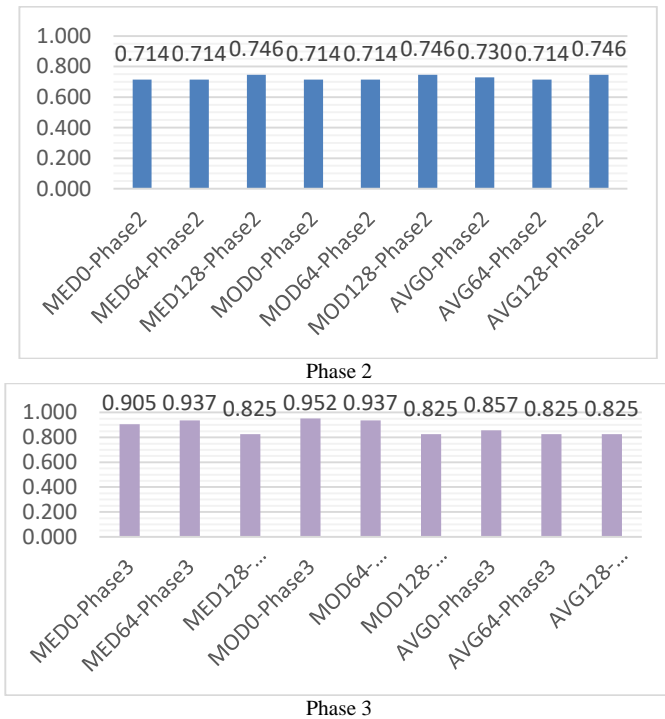


Fig. 6. Average precision for label prediction on test images belonging to (a) Phase 2 and (b) Phase 3. We used different metrics (i.e., Median, Mod and Average) on the training set to determine LBOUND and UBOUND.

Based on the results shown in Fig. 6, the optimal combinations for Phase 2's images are MED128, MOD128, and AVG128, with average label prediction precision of 74.6%. Evidently, setting a strict threshold value to reject non-zero cells with weak intensity is the best approach for Phase 2's images. A hue-saturation combination is retained only if it has a high occurrence inside the image.

Phase 3 returns a higher top precision value, i.e., 95.2%. This is expected since contamination (or none) will become more apparent in a latter phase. The high precision value validates our method of basing the label prediction on non-zero cell count (i.e., entropy measure). Unlike Phase 2, a relaxed threshold value returns the best result. The optimal combination is MOD0.

2) *Rhizomorph mycelium contamination recognition growth analysis measurement*: We measure the growth of the cultivation by phase prediction using the same test set, but only on the NON-CONTAMINATED specimens. The results are shown in Fig. 7. The highest average precision of 50.5% is obtained using MOD0. The lowest average precision of 34.9% is obtained using MOD128. The precision of random classification by chance is 33.3% (i.e., 1/3). The low precision is due to the specimens each exhibiting a different growth rate, especially from Phase 2 onwards. Table II shows the average precision achieved using MOD0, for different phases.

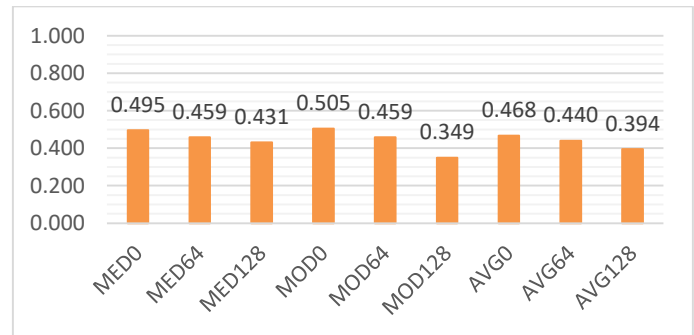


Fig. 7. Average precision for phase prediction on test images. We used different metrics (i.e., Median, Mod and Average) on the training set to determine LBOUND and UBOUND.

TABLE II. AVERAGE PRECISION ACHIEVED USING MOD0 FOR PHASE 1, PHASE 2 AND PHASE 3

PHASE	Number of Images	Average Precision
PHASE 1	47	87.2%
PHASE 2	31	32.3%
PHASE 3	31	32.3%
Average:		50.5%

Fig. 8 shows the training and testing loss for both MConNet and MNet models. While the disparity may not be readily apparent, it is evident that MConNet exhibits lower loss compared to the MNet model. Fig. 9 shows the training and testing accuracy for both MConNet and MNet models. Based on these graphs, even though the difference is not that obvious, MConNet has a higher accuracy performance compared to the MNet model.

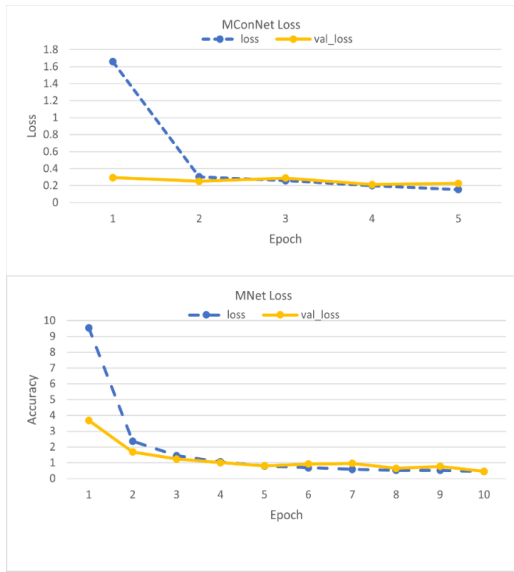


Fig. 8. Loss graph for MConNet and MNet.

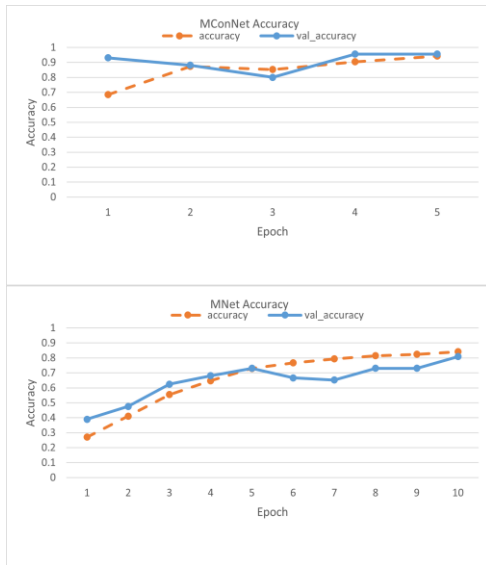


Fig. 9. Accuracy graph for MConNet and MNet.

B. Classification using CNN-based Method

1) *Rhizomorph mycelium contamination recognition:* Table III shows the accuracy percentage for contamination recognition. According to the mushroom experts' opinion, strain B has several contaminated Petri dishes. The method that has been used managed to recognize the contaminated samples from strain B which is 100%. Overall, the average accuracy for good and contaminated Petri dishes is more than 96%.

TABLE III. CONTAMINATION RECOGNITION

	Good	Contaminated
Strain A	95.66%	92.62%
Strain B	97.74%	100%
Average	96.64%	98.97

2) *Growth analysis measurement:* Tables IV and V shows the mycelium phase recognition for two different strains. The average recognition for strain A is 98.3% while 86% for strain B. The accuracy for mycelium phase recognition for strain A is much higher compared to strain B since the petri dish with strain B has more contaminated mycelium. The recognition of the phase for strain B is much harder, especially when at phase 2. This is because mycelium has become more like contaminated ones during phase 2.

TABLE IV. MYCELIUM PHASE RECOGNITION FOR STRAIN A

Samples/ Phases	Day 1 - Day 5	Day 6 - Day 9	Day 10 - Day 14
Day 1 - Day 5	100%	1%	
Day 6 - Day 9		99%	4%
Day 10 - Day 14			96%

TABLE V. MYCELIUM PHASE RECOGNITION FOR STRAIN B

Samples/ Phases	Day 1 - Day 5	Day 6 - Day 9	Day 10 - Day 14
Day 1 - Day 5	93%		
Day 6 - Day 9	4%	65%	
Day 10 - Day 14	3%	35%	100%

VI. CONCLUSION

This paper aims to introduce a machine learning approach for detecting rhizomorph mycelium growth and distinguishing between healthy and contaminated mycelium based on captured images. The results demonstrate that the employed method exhibits a notable accuracy in identifying healthy and contaminated mycelium. However, the study's scope is constrained by reduced precision beyond the initial five days, stemming from differing growth rates.

For our future work, we would like to explore the possibility of predicting rhizomorph growth from the area that it covered in a petri dish. Based on the area covered by the mycelium, we can predict the growth of such mycelium. In addition, we plan to use another type of mushroom in the experiment. We would like to see whether the growth can be measured easily compared to oyster mushroom.

ACKNOWLEDGMENT

This research is fully supported by Universiti Malaysia Sarawak through Smart Partnership Grant Scheme F08/PARTNERS/2128/2021. The authors fully acknowledged Universiti Malaysia Sarawak for the approved fund which makes this important research viable and effective. The acknowledgment is also extended to our industry counterpart, Madam Nurhaida Sahera Abd Malek who is willing to share the strain from Arra Mushroom Sdn Bhd, farm.

REFERENCES

[1] Borah, Tasvina, Singh, Akoijam Paul, Pampi, Talang, Hammylliende & Kumar, Bagis and Hazarika, Samarendra. "Spawn Production and Mushroom Cultivation Technology", ICAR Research Complex for NEH Region, Meghalaya, India (2019), pp. 1-46.

[2] Yafetto L, "The structure of mycelial cords and rhizomorphs of fungi: A mini-review". Mycosphere 9(5), 984-998, 2018. Doi 10.5943/mycosphere/9/5/3.

- [3] Katel, Shambhu, Mandal, Honey and Sharma, Rohit. "Oyster Mushroom Cultivation", in Research Trends in Agriculture Sciences, 30th Edition, Chapter: 3, AkiNik Publications, 2022, pp.39-56.
- [4] Ottom, Mohammad Ashraf and Alawad, Noor Aldeen. "Classification of mushroom fungi using machine learning techniques". International Journal of Advanced Trends in Computer Science and Engineering, 8(5), September - October 2019, pp.2378- 2385. DOI://10.30534/ijatcse/2019/78852019.
- [5] Preechasuk, Jitdumrong, Chaowalit, Orawan and Pensiri, Fuangfar and Visutsak, Po- rawat, "Image analysis of mushroom types classification by convolution neural networks", 2019, pp.82-88. 10.1145/3375959.337598.
- [6] Maurya, P. and Singh, N.P., "Mushroom classification using feature-based machine learning approach". In: Chaudhuri, B., Nakagawa, M., Khanna, P., Kumar, S. (eds) Proceedings of 3rd International Conference on Computer Vision and Image Processing. Advances in Intelligent Systems and Computing, vol 1022. Springer, Singapore. 2020. https://doi.org/10.1007/978-981-32-9088-4_17.
- [7] N. Zahan, M. Z. Hasan, M. A. Malek and S. S. Reya, "A deep learning-based approach for edible, inedible and poisonous mushroom classification," 2021 International Conference on Information and Communication Technology for Sustainable Development (ICICT4SD), Dhaka, Bangladesh, pp. 440-444, 2021, doi: 10.1109/ICICT4SD50815.2021.9396845.
- [8] Paudel, Nawaraj and Bhatta, Jagdish, "Mushroom classification using random forest and REP tree classifiers", Nepal Journal of Mathematical Sciences. 3, pp. 111-116, 2022. 10.3126/njmathsci.v3i1.44130.
- [9] Viswanadham, S., Muttipati, A.S., Lakshmi, N.J., Sujatha, Y., "Mushroom classification and feature extraction using linear discriminant analysis". In: Bhateja, V., Khin Wee, L., Lin, J.CW., Satapathy, S.C., Rajesh, T.M. (eds) Data Engineering and Intelligent Computing. Lecture Notes in Networks and Systems, vol 446, Springer, Singapore, 2022. https://doi.org/10.1007/978-981-19-1559-8_34.
- [10] S. K. Pal, R. Pant, R. Roy, S. Singh, L. Choudhary and S. Naaz, "Mushroom classification model to check edibility using machine learning," 2023 10th International Conference on Computing for Sustainable Global Development (INDIACom), New Delhi, India, 2023, pp. 214-217.
- [11] M. R. M. Kassim, I. Mat and I. M. Yusoff, "Applications of Internet of Things in mushroom farm management," 2019 13th International Conference on Sensing Technology (ICST), Sydney, NSW, Australia, 2019, pp. 1-6, doi: 10.1109/ICST46873.2019.9047702.
- [12] A. A. Shakir, F. Hakim, M. Rasheduzzaman, S. Chakraborty, T. U. Ahmed and S. Hossain, "Design and Implementation of SENSEP ACK: an iot based mushroom cultivation monitoring system," 2019 International Conference on Electrical, Computer and Communication Engineering (ECCE), Cox's Bazar, Bangladesh, 2019, pp. 1-6, doi: 10.1109/ECACE.2019.8679183.
- [13] Pramod, Mathew, Jacob., Jeni, Moni., Sneha, Sunil, "An intelligent system for cultivation and classification of mushrooms using machine vision", 2023 International Conference on Computational Intelligence and Sustainable Engineering Solutions (CISES), Greater Noida, India, 2023, pp. 264-270, doi: 10.1109/CISES58720.2023.10183464.
- [14] Md. Ariful Islam, Md. Antonin Islam, Md Saef Ullah Miah, and Abhijit Bhowmik, "An automated monitoring and environmental control system for laboratory-scale cultivation of oyster mushrooms using the Internet of Agricultural Thing (IoAT)". In Proceedings of the 2nd International Conference on Computing Advancements (ICCA '22). Association for Computing Machinery, New York, NY, USA, 200, pp.207–212. <https://doi.org/10.1145/3542954.3542985>.
- [15] A. Anil, H. Gupta and M. Arora, "Computer vision based method for identification of freshness in mushrooms," 2019 International Conference on Issues and Challenges in Intelligent Computing Techniques (ICICT), Ghaziabad, India, 2019, pp. 1-4, doi: 10.1109/ICICT46931.2019.8977698.
- [16] Ma, Y., Xia, Y., & He, X, "A preliminary study on mushroom classification and application of SVM principle to infer the linearly separable dataset". In Advances in Petrochemical Engineering and Green Development, 2022, pp. 470-476, CRC Press.
- [17] Cucut, Hariz, Pratomo., Widyastuti, Andriyani, "Mushroom image classification using C4.5 algorithm". Journal of Intelligent Software System, 2(1), pp.17-19, 2023. doi: 10.26798/jiss.v2i1.930.
- [18] Zheng, Y.-Y.; Kong, J.-L.; Jin, X.-B.; Wang, X.-Y.; Su, T.-L.; Zuo, M. "CropDeep: The crop vision dataset for deep-learning-based classification and detection in precision agriculture". Sensors 2019, 19, 1058. <https://doi.org/10.3390/s19051058>.
- [19] L. Boukhris, J. Ben Abderrazak and H. Besbes, "Tailored deep learning based architecture for smart agriculture," 2020 International Wireless Communications and Mobile Computing (IWCMC), Limassol, Cyprus, 2020, pp. 964-969, doi: 10.1109/IWCMC48107.2020.9148182.
- [20] Yingyuan Du, Tao Wu, Gaoyuan Yang, Yuwei Yang, Ge Peng, "Classification algorithm based on convolutional neural network for wild fungus", Third International Conference on Artificial Intelligence and Computer Engineering (ICAICE 2022); 126105D (2023) <https://doi.org/10.1117/12.2671050>.